Int. J. Electrochem. Sci., 16**(2021)** Article Number: 211026, doi: 10.20964/2021.10.35

International Journal of ELECTROCHEMICAL SCIENCE
www.electrochemsci.org

Short Communication

Crack-free Sol-Gel Coatings for Corrosion Protection of Carbon steel in concrete pore solution: An electrochemical corrosion investigation

Meng Zhang

Architectural Engineering Institute, Chongqing Industry Polytechnic College, Chongqing 401120, China
E-mail: zhangmengcq2020@163.com

Received: 12 June 2021/ *Accepted:* 30 July 2021 / *Published:* 10 September 2021

In this work, an appropriate protective coating for rebar has been discovered to increase the durability of such buildings when exposed to harsh environments. Electrochemical measurements were used to study the corrosion behavior of crack-free sol-gel coating carbon steel rebar in concrete pore solution containing chloride ions. Polyvinyl butyral (PVB)/silica (PVB/silica) nanocomposites were synthesized as hybrid sol-gel coatings on carbon steel rebar. Electrochemical impedance spectroscopy and polarization measurements were used to assess the corrosion resistance of coatings. The mechanical result indicates that Young's modulus improved from 36.3 for pure PVB to 94.5 MPa for the PVB containing 15wt% silica. The electrochemical results indicate that an optimal PVB containing 10wt% silica-coated on steel rebar was required for the best performance of corrosion resistance. After two days of exposure, the coated PVB/10silica in CPS showed an inhibitory efficiency of 89.3%, which is highly good when compared to several recent publications.

Keywords: Electrochemical corrosion; Sol-Gel Coatings; Carbon steel rebar; Concrete pore solution

1. INTRODUCTION

Reinforced concrete, pipelines, and machinery framing are just a few of the industries that use carbon steel [1-3]. Carbon steel corrosion is a devastating phenomenon that affects countless infrastructures [4-6]. Repair of reinforced concrete requires $200/m² of exposed surface in concrete applications [7, 8]. The annual cost for concrete corrosion in bridge structures in the United States is $8.3 billion, which includes maintenance, replacement, and construction expenses. Corrosion of reinforced concrete is usually difficult to detect because the steel's surface can rust and degrade while hidden underneath the concrete [9, 10]. The uncertainty of concrete corrosion shows that steel reinforcement has to be better protected. The impacts of surface treatment by unmodified sol-gel and

polyvinyl butyral (PVB)/silica (PVB/silica) modified sol-gel coatings on corrosion behavior of the carbon steel is examined in this work.

PVB is a strong and flexible material. It's noted for its great influence strength at low temperatures, in particular [11-13]. PVB also has good adhesive qualities with a variety of materials, including wood, metal, plastics, and glass. PVB is therefore frequently used as a printing paste, an adhesive agent, a paint, and a film sandwiched in a car's safety glass [14, 15]. Due to PVB's excellent adhesive capability, a nanocomposite of PVB with glass might be made using the sol-gel method. The characteristics of PVB should alter and its functions should develop if the glass is mixed with it [16, 17]. Fu et al. synthesized a silica/PVB hybrid material, which they utilized to enable ternary ferric oxide compounds and phenanthroline [18, 19]. However, the hybrid's electrochemical characteristics of PVB/silica-coated steels have not been reported. The corrosion behavior of PVB/silica nanocomposites generated by the sol-gel technique will be discussed in this research.The corrosion resistance of coated carbon steel rebar in an aggressive environment was investigated using polarization analysis and electrochemical impedance spectroscopy (EIS).

2. MATERIALS AND METHOD

In order to prepared coating materials, tetrabutylammonium hydroxide (TBAOH), tetraethylammonium hydroxide (TEAOH), tetraethyl orthosilicate (TEOS), polyvinyl butyral, $NaAlO_2$, and were purchased from Sinopharm Chemical Reagent Company (China). PVB was added to 30 g of alcohol at a rate of 4g per 30g of alcohol. PVB was completely dissolved before 40g of TEOS was added to the alcohol solution. The PVB and TEOS were fully combined with a magnetic stirrer. The alcohol solution of TEOS and PVB was then dropwise added to a solution of $NaAlO_2$ (1g) and TEAOH (40g, 25%). In just a few minutes, the TEOS was hydrolyzed, yielding a homogenous PVB/silica composite. To evaporate the alcohol, the suspension was agitated in the open air overnight. In this study, PVB composite was mixed with different silica content such as 0wt% silica, 5wt% silica, 10wt% silica, and 15wt% silica which are indicated as PVB, PVB/5silica, PVB/10silica, and PVB/15silica, respectively. The prepared gel was deposited by dip-coating onto carbon steel rebar, having the chemical compositions (wt.%) 0.076 C, 0.032 Si, 0.28 Mn, 0.017 P, 0.032 S, 0.017 Cr, 0.014 Ni, 0.011 Mo, 0.027 Cu, 0.027 Al, and balance Fe. To achieve a uniform smooth surface, the samples were polished with class-600 silicon carbide sandpaper, then washed with double pure water and thoroughly rinsed with acetone. After that, the carbon steel was immersed in the prepared solution, removed at a rate of 14 mm/min, and air-dried for about 10 minutes. This method was repeated twice, following which the coated steel rebars were preheated for 24 hours at 65 degrees Celsius and cured for 3 hours at 150^{o}C.

In concrete pore solution (CPS) containing chloride ions, electrochemical characterization was carried out. The CPS was made by adding 11.22 g of KOH to 1L of a saturated $Ca(OH)_2$ solution, resulting in solutions with a final pH of 13.2. Gamry Interface 1010 Potentiostat was employed, as well as a typical three-electrode cell arrangement. A saturated calomel electrode, a graphite rod and coated carbon steel rebar were used as a reference electrode, a counter electrode and a working electrode,

respectively. With a voltage of 10 mV, EIS was conducted at OCP between the frequencies of 1mHz and 1MHz. Finally, the polarization test was done by a scan rate of 0.1mV/s.

3. RESULTS AND DISCUSSION

The mechanical characteristics derived from the stress-strain plots for every sample are shown in Table 1. PVB/15silica has Young's modulus that is around 2.6 times that of pure PVB. While Young's modulus of the poly(vinyl alcohol)(PVA)/silica composite [20] rises from 31.8MPa for pure PVA to 45.2MPa for a 15 wt% silica nanocomposite. It's a 1.4-time rise. As a result, the SiO_2 particles are thought to distribute effectively in the PVB polymer matrix. With increasing silica concentration, yield stress increases as well, although elongation at break reduces.

Table 1. Mechanical characteristics of coated carbon steel rebars

Coating materials	Yield stress(MPa)	Young's modulus(MPa)	Elongation at break(%)
PVB	378.4	36.3	4.7
PVB/5silica	641.7	59.6	3.8
PVB/10silica	822.9	76.8	3.2
PVB/15silica	1012.1	94.5	2.6

Once coatings are included, EIS is a strong technique that is often used to monitor and forecast corrosion processes. As illustrated in Figure 1, the data collected by the EIS experiments may be replicated by numerical fitting with ZipWin software utilizing the best fit equivalent circuits (Fig. 2).

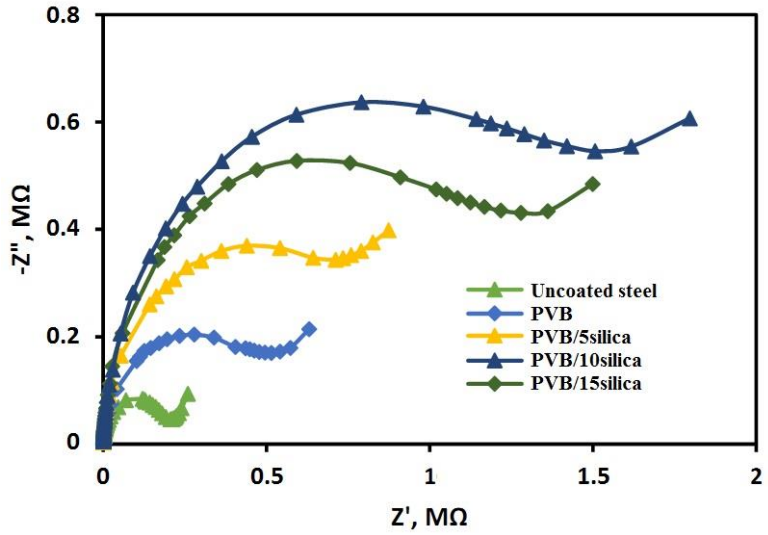

Figure 1. Nyquist plots of coated carbon steel rebars after 2 hours of immersion in concrete pore solution in frequency range of 1mHz and 1MHz at room temperature.

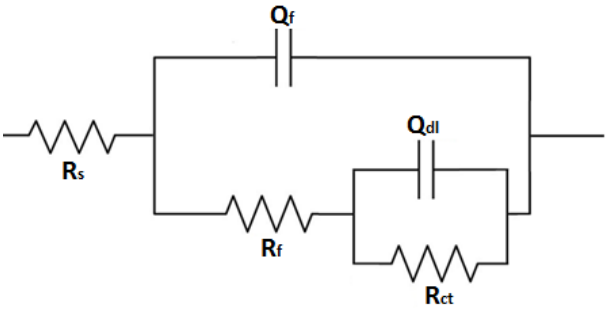

Figure 2. A fitted circuit model

Impedance investigations and data manipulations reveal impedance parameters such as solution resistance (R_s), charge-transfer resistance (R_{ct}), coating resistance (R_f), the electric double-layer capacitance at the steel/electrolyte interface (Q_{dl}), and coating capacitance (Q_f) [21].The R_{ct} can be used to predict the corrosion behavior of the samples, proving the corrosion resistance in an aggressive environment. It becomes increasingly difficult to react as the charge-transfer impedance rises. In addition, the R_{ct} was inversely related to the defects in the steel coating material. Two different charge layers on the material surface formed the double layer capacitance, Qdl. Table 2 shows the electrochemical parameters. The inhibition efficiency (η) can be determined by the following equation:

$$\eta(\%) = 100\times(R_{ct} - R_{ct}^*)/R_{ct} \quad (1)$$

where R_{ct} represents the charge-transfer resistance of the coated steels and Rct* indicates the charge-transfer resistance of uncoated steel. As shown in Table 2, the R_{ct} values of the coated steel were greater than that of the naked steel, indicating that the coating has a longer barrier property and is more resistant to corrosion in the CPS environment. PVB/silica coating enhanced coating resistance and charge-transfer resistance of coated carbon steel. A low coating capacitance (0.4 μF/cm^2) and high Rct (2.16 MΩ cm^2) value was found by PVB/10silica coating in comparison to uncoated sample and record an inhibition efficiency (η) of 89.3%. The findings validate the theory that increasing the amount of silica in the PVB coating material from 5 to 15 wt% improved corrosion inhibition performance and efficiency. However, when 10wt% silica was used, the inhibition efficiency indicated a reverse tendency. This can be deduced that an optimal silica load is required to improve the steel's corrosion resistance properties, whereas higher loading results in the formation of a breakable layer with poor barrier properties, which could be due to the development of enhanced defects on the shaped sol-gel layer. As a result, in this work, an optimum of 15wt% silica is determined in PVB, resulting in increased protection efficiency.

Table 2. EIS parameters resulting from circuit model for coated carbon steel rebar

Coating materials	R_s(Ω cm^2)	R_f(MΩ cm^2)	Q_f(μF cm^{-2})	R_{ct}(MΩ cm^2)	Q_{dl}(μF cm^{-2})	η(%)
Uncoated steel	75	0.11	1.5	0.23	2.2	-
PVB	71	0.28	1.1	0.72	1.5	68.0
PVB/5silica	82	0.59	0.7	1.13	1.1	79.6
PVB/10silica	78	1.51	0.4	2.16	0.7	89.3
PVB/15silica	73	1.12	0.5	1.72	0.9	86.6

Table 3 compares the efficacy of samples with various coating materials as described in the literature. The findings showed that the η of the PVB/10silica sample for steel corrosion resistance was comparable to those found in the literature.

Table 3. ηof samples with various coating materials as described in the literature

Coating materials	**Environment**	**η(%)**	**Ref.**
Epoxy Coating	3.5wt% NaCl	66.3	[22]
Polyester polyol-aromatic isocyanate	3wt% NaCl	46.1	[23]
PVA and Titania	3.5wt% NaCl	97.9	[24]
Organic–inorganic hybrid	CPS	64.5	[25]
PVB/10silica	CPS	89.3	This work

Polarization experiments have long been used to monitor the capacity of metal substrates in harsh corrosion environments. Figure 3 shows the Tafel plots of coated and uncoated carbon steel rebars after 2 hours of immersion in CPS. When compared to bare carbon steel, both anodic and cathodic Tafel plots reveal a significant shift to smaller current densities for those coated specimens. The inhibition efficiency (η) can be determined by the following equation:

$$\mu(\%) = 100 \times (i_{corr} - i_{corr}^*)/i_{corr} \quad (2)$$

where i_{corr}^* and i_{corr} present the values of corrosion current density of uncoated and coated carbon steel rebars, respectively. Table 4 lists electrochemical corrosion parameters such as inhibition efficiency (η), corrosion current density (I_{corr}), corrosion potential (E_{corr}), and extrapolated Tafel slopes such as βa and βc. These findings indicate that I_{corr} reduced as the concentration of silica in PVB coating materials increased, providing strong support for the coated steel surface's extended protective nature. The I_{corr} of PVA/10silica was 0.09mA/cm^2, which was much lower than that of bare carbon steel (1.8mA/cm^2). For PVB, PVB/5silica, PVB/10silica and PVB/15silica, the η(%) achieved is 55.5, 83.3, 95.0, and 88.9, respectively. These results are quite comparable to those obtained using impedance studies, which is a completely different methodology with a higher risk of mistake [26-29].

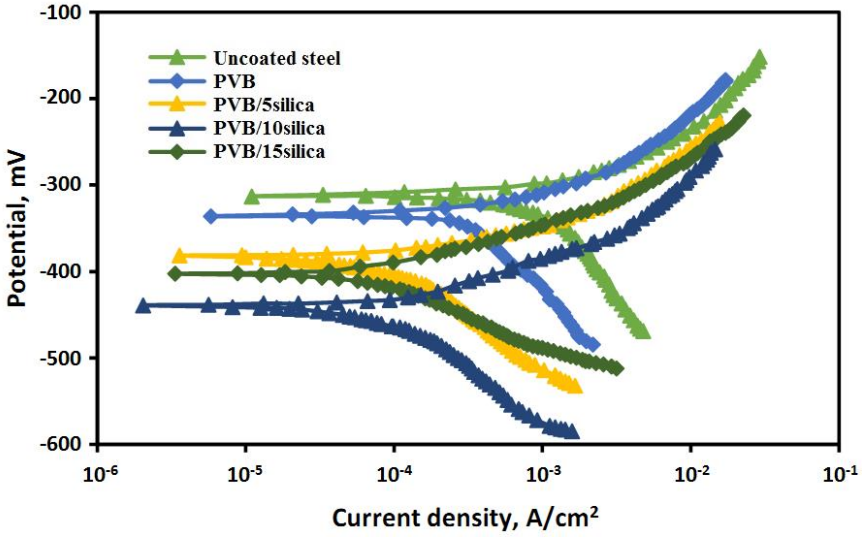

Figure 3. Potentiodynamic polarization curves of coated and uncoated carbon steel rebars after 2 hours of immersion in concrete pore solution at 0.1mV/s scanning rate at room temperature

Table 4. The electrochemical corrosion parameters derived from Fig. 3

Coating materials	Corrosion current density (mA/cm^2)	Corrosion potential (mV)	$-\beta_c$ ($mVdec^{-1}$)	β_a ($mVdec^{-1}$)	μ(%)
Uncoated steel	1.8	-317	69	145	-
PVB	0.8	-336	37	174	55.5
PVB/5silica	0.3	-382	44	168	83.3
PVB/10silica	0.09	-432	61	123	95.0
PVB/15silica	0.2	-401	58	154	88.9

The creation of a Si-O-Si sol-gel network is caused by the hydrolysis and condensation processes of silicon methoxide. Because silica has a significant number of -OH groups on its surface, it may form bonds with PVB via a condensation process [30]. During the sintering process, these weak connections were converted into stable covalent bonds. Chemical bonding allows the PVA/silica mixture to adhere to the metal surface quite well. The successful blocking of corrosion might be attributed to the Si–O–Si linkage, as well as the Fe–Si–O connection and compactness of the covered surface.

The surface morphologies of the bare carbon steel and PVB/10silica coated steel rebars are shown in Fig. 4. The surface of the PVB/10silica sample was nearly uniform, with little indications of defects/pores or roughness, which might reduce the impact of corrosive ions and water from the CPS on the metal surface.

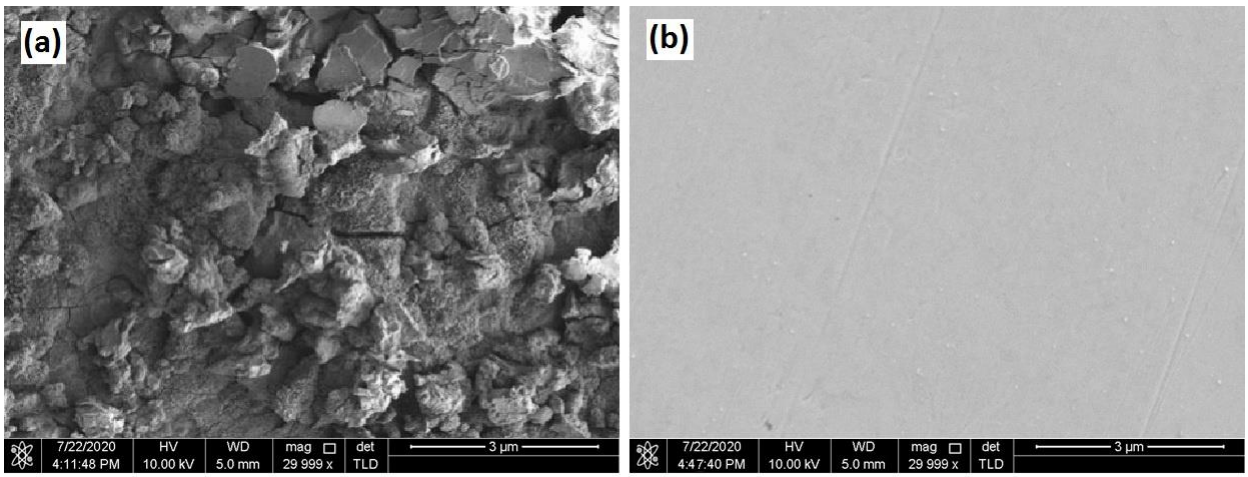

Figure 4. The surface morphologies of (a) the bare carbon steel and (b) PVB/10silica coated steel rebars after 2 hours of immersion in concrete pore solution at room temperature

4. CONCLUSIONS

Electrochemical measurements were used to study the corrosion behavior of crack-free sol-gel coating carbon steel rebar in concrete pore solution containing chloride ions. PVB/silica nanocomposites were synthesized as hybrid sol-gel coatings on carbon steel rebar. Electrochemical impedance spectroscopy and polarization measurements were used to assess the corrosion resistance of coatings. The mechanical result indicates that the Young's modulus improved from 36.3 for pure PVB to 94.5 MPa for the PVB containing 15wt% silica. The electrochemical results indicate that an optimal PVB containing 10wt% silica-coated on steel rebar was required for the best performance of corrosion resistance. After two days of exposure, the coated PVB/10silica in CPS showed an inhibitory efficiency of 89.3%, which is highly good when compared to several recent publications. SEM analysis of the corroded surface of carbon steel in presence of PVB/10silica indicates the decrease of corrosion.

ACKNOWLEDGEMENT
This study was supported by the Science and Technology Research Program of Chongqing Municipal Education Commission (Grant No.KJQN201803205).

References

1. F. Rubino, A. Nisticò, F. Tucci and P. Carlone, *Journal of Marine Science and Engineering*, 8 (2020) 26.
2. C.S. Kumar, V.S. Rao, V. Raja, A. Sharma and S. Mayanna, *Corrosion Science*, 44 (2002) 387.
3. S. Kakooei, H.M. Akil, A. Dolati and J. Rouhi, *Construction and Building Materials*, 35 (2012) 564.
4. Y. Liu, Z. Wang and Y. Wei, *International Journal of Electrochemical Science*, 14 (2019) 1147.

5. Y. Li, D.D. Macdonald, J. Yang, J. Qiu and S. Wang, *Corrosion Science*, 163 (2020) 108280.
6. X. Li, T. Shi, B. Li, X. Chen, C. Zhang, Z. Guo and Q. Zhang, *Materials & Design*, 183 (2019) 108152.
7. N.T.K. Al-Saadi, A. Mohammed, R. Al-Mahaidi and J. Sanjayan, *Construction and Building Materials*, 209 (2019) 748.
8. L. Sun, C. Li, C. Zhang, Z. Su and C. Chen, *International Journal of Structural Stability and Dynamics*, 18 (2018) 1840001.
9. P. Wang, H. Qiao, Y. Li, Q. Feng and K. Chen, *Structural Concrete*, 21 (2020) 1905.
10. M. Abedini and C. Zhang, *Structural Engineering and Mechanics*, 77 (2021) 441.
11. Z. Ma, M. Sun, A. Li, G. Zhu and Y. Zhang, *Progress in organic coatings*, 144 (2020) 105662.
12. W. Zhang, Z. Tang, Y. Yang, J. Wei and P. Stanislav, *Journal of Structural Engineering*, 147 (2021) 04021055.
13. S. Kakooei, H.M. Akil, M. Jamshidi and J. Rouhi, *Construction and Building Materials*, 27 (2012) 73.
14. F. Ambrulevičius, A. Pulmanas, D. Plaušinaitis and V. Daujotis, *International Journal of Electrochemical Science*, 14 (2019) 441.
15. Y. Bai, S. Wang, B. Mou, Y. Wang and K.A. Skalomenos, *Engineering Structures*, 227 (2021) 111443.
16. Y.-X. Qiao, S.-L. Sheng, L.-M. Zhang, J. Chen, L.-L. Yang, H.-L. Zhou, Y.-X. Wang, H.-B. Li and Z.-B. Zheng, *Journal of Mining and Metallurgy, Section B: Metallurgy*, (2021) 25.
17. F. Guo, S. Wu, J. Liu, Z. Wu, S. Fu and S. Ding, *Engineering Fracture Mechanics*, 248 (2021) 107711.
18. L. Fu, H. Zhang, S. Wang, Q. Meng, K. Yang and J. Ni, *Journal of sol-gel science and technology*, 25 (2019) 49.
19. J. Zhu, Y. Chen, L. Zhang, B. Guo, G. Fan, X. Guan and R. Zhao, *Journal of Cleaner Production*, 295 (2021) 126405.
20. K. Nakane, T. Yamashita, K. Iwakura and F. Suzuki, *Journal of Applied Polymer Science*, 74 (2019) 133.
21. H. Castaneda and M. Galicia, *Frontiers in Materials*, 6 (2019) 307.
22. J. Ress, U. Martin, J. Bosch and D.M. Bastidas, *Coatings*, 11 (2021) 113.
23. R. Selvaraj, M. Selvaraj and S. Iyer, *Progress in organic coatings*, 64 (2009) 454.
24. P. Jaseela, M. Kuruvilla, L. Williams, C. Jacob, K. Shamsheera and A. Joseph, *Arabian Journal of Chemistry*, 13 (2020) 6921.
25. R.B. Figueira, C.J. Silva and E.V. Pereira, *Journal of Coatings Technology and Research*, 13 (2016) 355.
26. A. Mukhopadhyay and S. Sahoo, *European Journal of Environmental and Civil Engineering*, 17 (2021) 1.
27. D.K. Kamde and R.G. Pillai, *Corrosion*, 76 (2020) 843.
28. L. Qu, Q. Wang, S. Xu, N. Wang and Z. Shi, *Construction and Building Materials*, 295 (2021) 123682.
29. M. Wang, Z. Zhou, Q. Wang, Z. Wang, X. Zhang and Y. Liu, *Journal of Alloys and Compounds*, 811 (2019) 151962.
30. A. Najafi, F. Golestani-Fard, H. Rezaie and S.P. Saeb, *Ceramics International*, 47 (2021) 6376.